Supporting Information

Attraction and Actuation of Water Nanodroplets on $MoS_2/MoSe_2$ Lateral Heterostructure Films

Wei Si[1*], Hong Wang[1], Yanlin He[1], Yaye Song[2]

[1]Jiangsu Key Laboratory for Design and Manufacturing of Precision Medicine Equipment, School of Mechanical Engineering, Southeast University, Nanjing 211100, China

[2]College of Biological Science, University of Guelph, Guelph N1G 2W1, Canada

Table S1 and Table S2 are the adopted L-J potential parameters from other articles. Table S3 is the calculated L-J potential parameters by using the Lorentz-Berthelot mixing rules.

Table S1. Lennard-Jones interaction parameters for S-O, Se-O, and Mo-O [1]

Pair	Epsilon	Sigma
S-O	0.006 eV	3.17 Å
Se-O	0.009 eV	3.41 Å
Mo-O	0.002 eV	3.61 Å

Table S2. Lennard-Jones parameters for O [2]

Element	Epsilon	Sigma
O	0.00844 eV	3.61 Å

Table S3. Lennard-Jones parameters for S, Se, and Mo

Element	Epsilon (eV)	Epsilon (kcal/mol)	Sigma (Å)	R (Å)
S	0.004265	0.09835	2.799	3.1418
Se	0.009597	0.22131	3.279	3.6805
Mo	0.000474	0.01093	3.679	4.1295

Fig.S1 shows a system for theoretical calculations. In this system, a single water molecule is set on a pristine $MoS_2/MoSe_2$ film and a $MoS_2/MoSe_2$ film perforated with a pore in the central region. We control this water molecule to move along with Z axis, the value of $z \in [2.5, 17]$ is for water molecule on pristine film, and $z \in [-17, 17]$ is for water molecule on film with a pore dug.

Due to van der Waals interactions, water molecule cannot penetrate the pristine $MoS_2/MoSe_2$ film. Therefore, we manually created a pore in the film to investigate the interactions when water molecules pass through it.

Fig.S2 illustrates a special case. In this theoretical calculation, the orientation of water molecule was fixed, and they were allowed to pass through the aforementioned perforated film, followed by the calculation of interaction energies between water molecule and the film. Fig.S3 to Fig.S5 present the energy profiles of water molecules penetrating the film at different positions with their orientations taken into account. Specifically, water molecule was rotated by 0°, 90°, 180°, and 270° around the Y-axis. Meanwhile, during the Y-axis rotation, they were simultaneously rotated by 0°, 90°, 180°, and 270° around the Z-axis. In other words, 16 values were calculated at each step and then averaged.

Fig.S6 shows the simulation systems we applied to verify the characteristics of interaction energies illustrated by theoretical calculations.

Fig.S7 displays the simulation systems for contact angle measurement with TIP3P(CHARMM) water model. The wettability of MoS_2 and $MoSe_2$ was investigated by comparing their contact angle differences. We adopted the code provided by Wang, Y., et al. [3] to calculate the average mass density of water cluster within the stable stage (after 4.8 ns in Fig. S7b). Subsequently, seven boundary points of the nanodroplet were defined using Fiji ImageJ [4], from which the fitted value of angle C was obtained. The contact angle was determined by subtracting angle C from 180°.

Fig.S8 shows the results for contact angle measurement with TIP4P-seris water models.

Fig.S9 illustrates the interaction energies between TIP4P-seris water and the $MoS_2/MoSe_2$ film.

Fig.S10 illustrates the simulation model employed to investigate the enrichment and immobilization behavior of water nanodroplets.

Fig.S11 illustrates the simulation model employed to investigate the fission behavior of water nanodroplets.

Fig.S12 displays the pre-constructed structural models for the fabrication of the final gradient-tunable heterostructure film.

Fig.S13 is the process of building 2D $MoS_2/MoSe_2$ film.

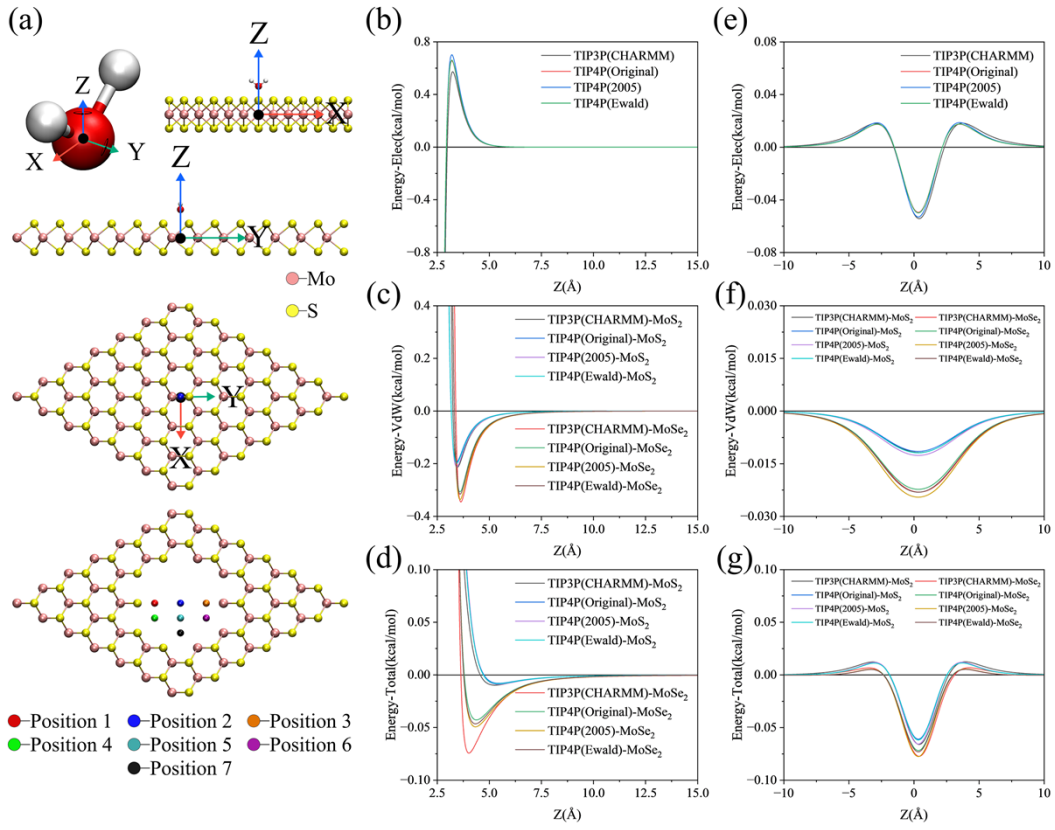

Fig.S1. Schematic diagram of the systems for theoretical calculations. (a) Schematic Diagram of one single water molecule on MoS_2 Film, there are two types of MoS_2 films, one with an pristine surface, and the other with a pore dug in the central region of the film. The same applies to $MoSe_2$ film. (b) Electrostatic interaction energies between water molecule and the pristine film at position 2 shown in Fig.S1.a. (c) Similar to panel b but for van der Waals interaction energies. (d) Similar to panel b but for total interaction energies. (e) Electrostatic interaction energies between water molecule and the film (perforated with a pore) at position 2 shown in Fig.S1.a, and water molecule can go through the film. (f) Similar to panel e but for van der Waals interaction energies. (g) Similar to panel e but for total interaction energies.

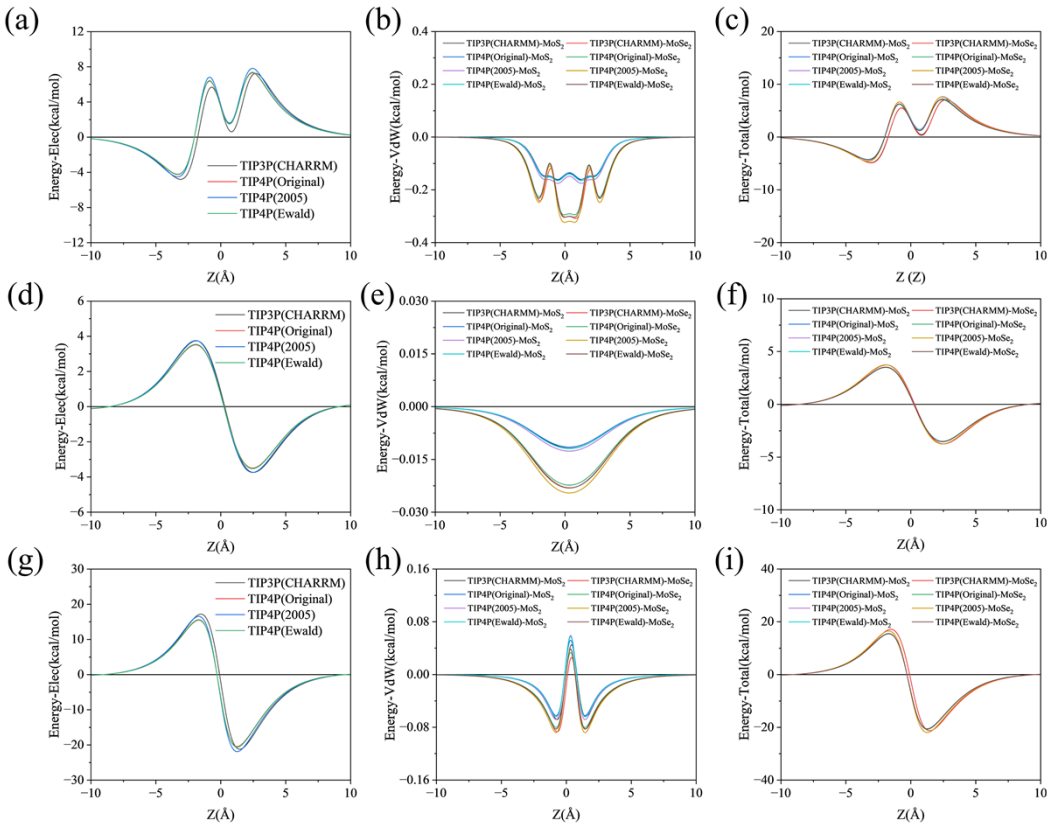

Fig.S2. Interaction energies of water molecule and MoS_2/$MoSe_2$ Film with no rotation of water molecule. (a) Electrostatic interaction energies between water molecule and MoS_2/$MoSe_2$ Film at position 1 shown in Fig.S1.a. (b) Similar to panel a but for Van der Waals interaction energies. (c) Similar to panel a but for total interaction energies. (d) Electrostatic interaction energies between water molecule and MoS_2/$MoSe_2$ film at position 2 shown in Fig.S1.a. (e) Similar to panel d but for van der Waals interaction energies. (f) Similar to panel d but for total interaction energies. (g) Electrostatic interaction energies between water molecule and MoS_2/$MoSe_2$ Film at position 3 shown in Fig.S1.a. (h) Similar to panel g but for van der Waals interaction energies. (i) Similar to panel g but for total interaction energies.

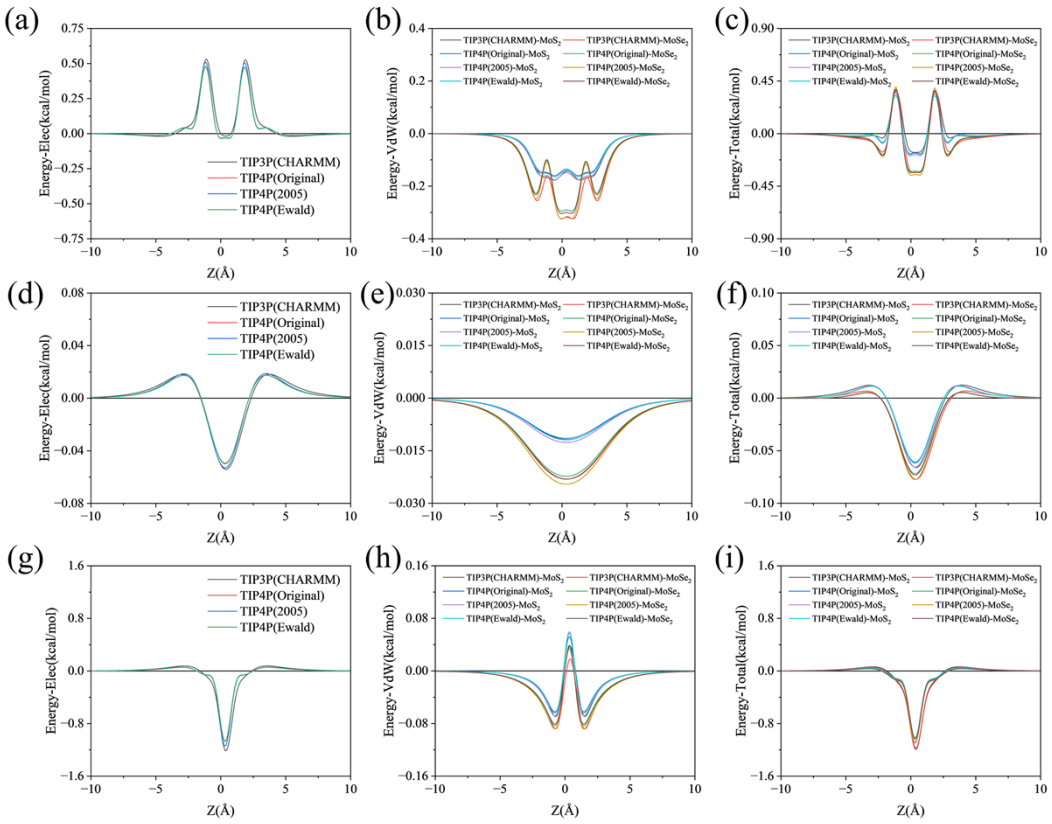

Fig.S3. Interaction energies of water molecule and MoS_2/$MoSe_2$ Film with rotation of water molecule. (a) Electrostatic interaction energies between water molecule and MoS_2/$MoSe_2$ Film at position 1 shown in Fig.S1.a. (b) Similar to panel a but for Van der Waals interaction energies. (c) Similar to panel a but for total interaction energies. (d) Electrostatic interaction energies between water molecule and MoS_2/$MoSe_2$ Film at position 2 shown in Fig.S1.a. (e) Similar to panel d but for van der Waals interaction energies. (f) Similar to panel d but for total interaction energies. (g) Electrostatic interaction energies between water molecule and MoS_2/$MoSe_2$ Film at position 3 shown in Fig.S1.a. (h) Similar to panel g but for van der Waals interaction energies. (i) Similar to panel g but for total interaction energies.

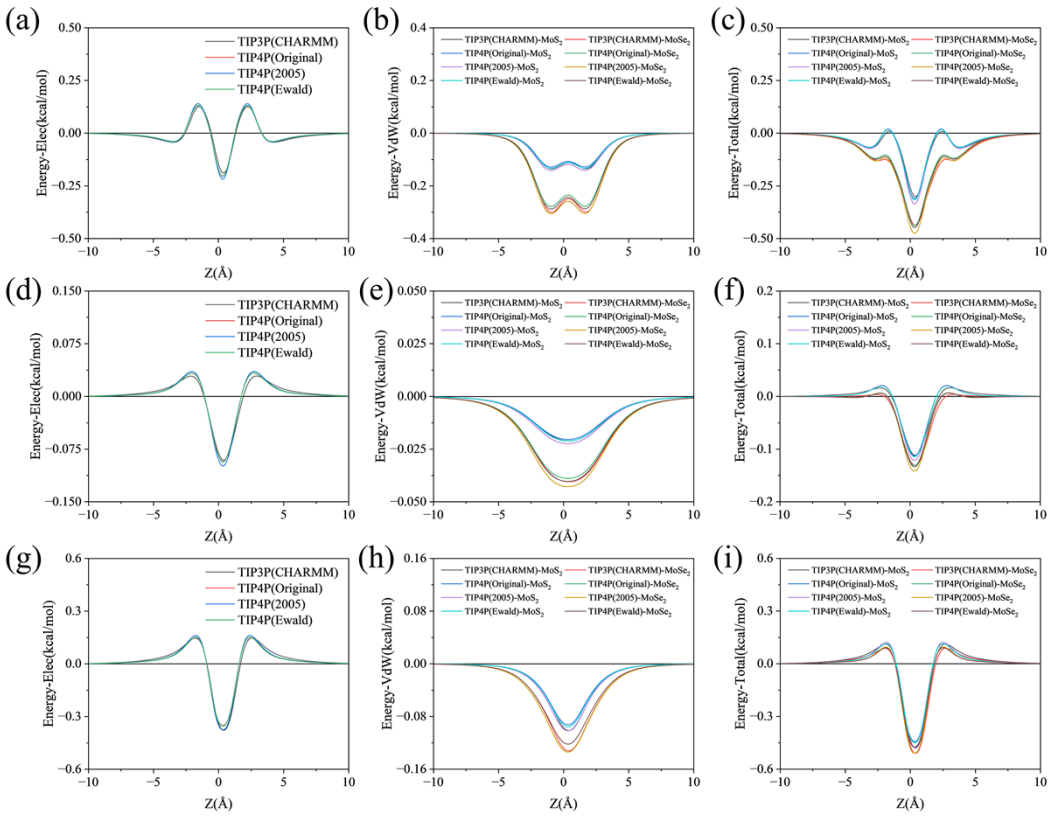

Fig.S4. Interaction energies of water molecule and MoS_2/$MoSe_2$ Film with rotation of water molecule. (a) Electrostatic interaction energies between water molecule and MoS_2/$MoSe_2$ Film at position 4 shown in Fig.S1.a. (b) Similar to panel a but for Van der Waals interaction energies. (c) Similar to panel a but for total interaction energies. (d) Electrostatic interaction energies between water molecule and MoS_2/$MoSe_2$ Film at position 5 shown in Fig.S1.a. (e) Similar to panel d but for van der Waals interaction energies. (f) Similar to panel d but for total interaction energies. (g) Electrostatic interaction energies between water molecule and MoS_2/$MoSe_2$ Film at position 6 shown in Fig.S1.a. (h) Similar to panel g but for van der Waals interaction energies. (i) Similar to panel g but for total interaction energies.

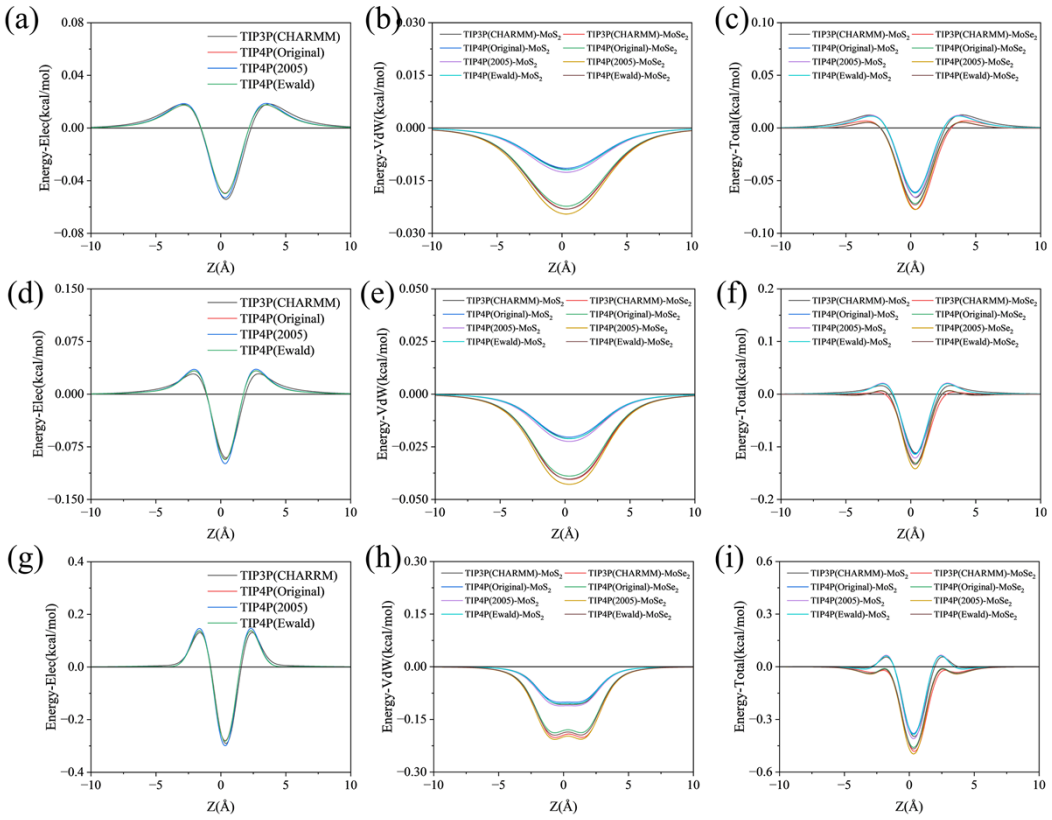

Fig.S5. Interaction energies of water molecule and MoS_2/$MoSe_2$ Film with no rotation of water molecule. (a) Electrostatic interaction energies between water molecule and MoS_2/$MoSe_2$ Film at position 2 shown in Fig.S1.a. (b) Similar to panel a but for Van der Waals interaction energies. (c) Similar to panel a but for total interaction energies. (d) Electrostatic interaction energies between water molecule and MoS_2/$MoSe_2$ Film at position 5 shown in Fig.S1.a. (e) Similar to panel d but for van der Waals interaction energies. (f) Similar to panel d but for total interaction energies. (g) Electrostatic interaction energies between water molecule and MoS_2/$MoSe_2$ Film at position 7 shown in Fig.S1.a. (h) Similar to panel g but for van der Waals interaction energies. (i) Similar to panel g but for total interaction energies.

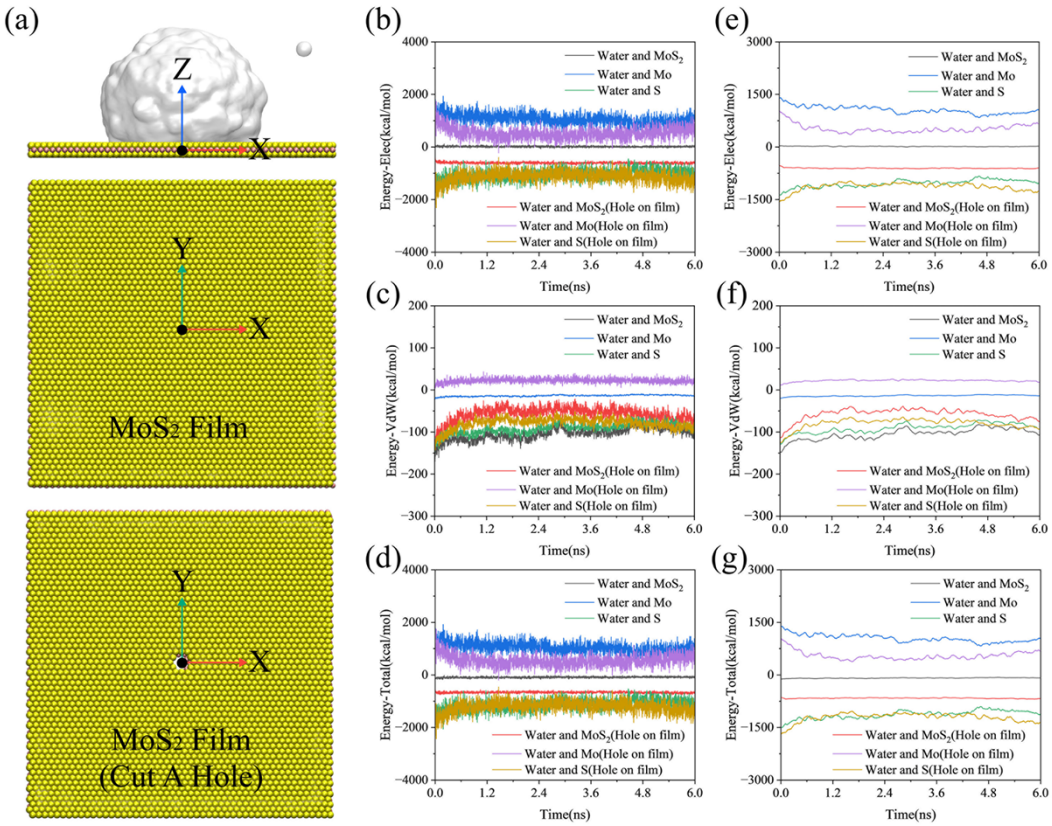

Fig.S6. Verification of the characteristics of interaction energies between water molecules and MoS_2 film. (a) Schematic diagram of the simulation systems, there are two types of MoS_2 films, one with an pristine surface, and the other with a pore of 1 nm diameter dug in the central region of the film. (b) The electrostatic interaction energies between water molecules and the films, Mo atom, and S atom. (c) Similar to panel b but for van der Waals interaction energies. (d) Similar to panel b but for total interaction energies. (e) Smoothed data of panel b. (f) Smoothed data of panel c. (g) Smoothed data of panel d.

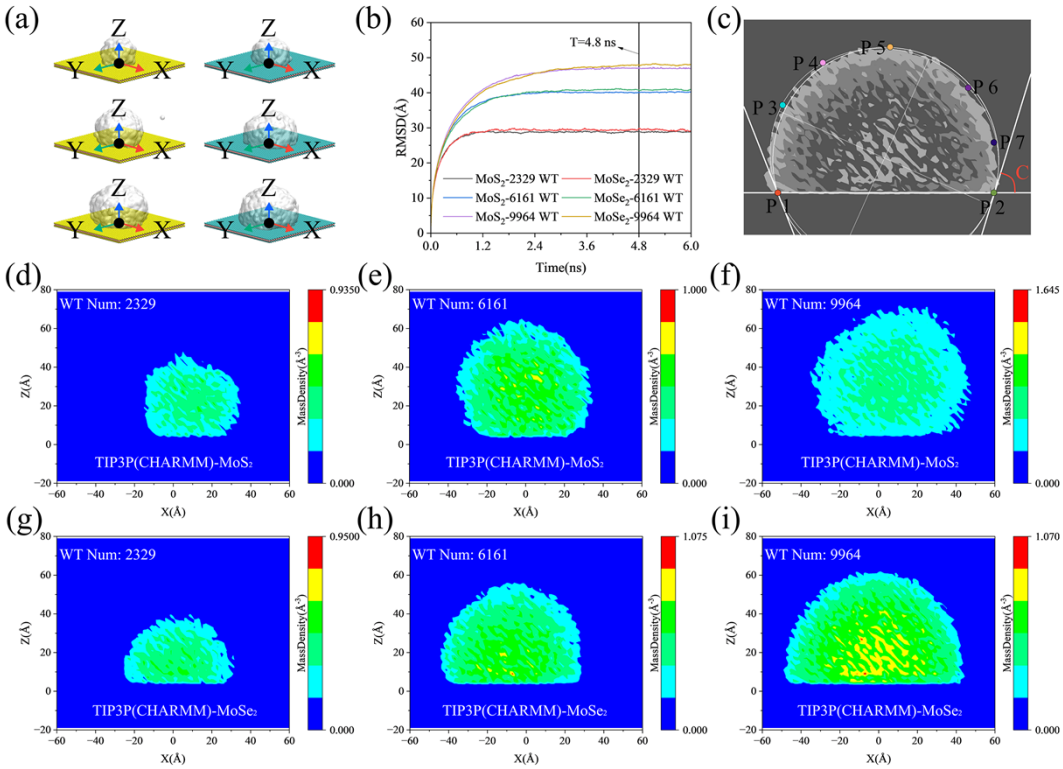

Fig.S7. Measurement of contact angle with TIP3P(CHARMM) water model. (a) Schematic diagram of nanodroplets with different number of water molecules on MoS_2 and $MoSe_2$ Films. (b) The RMSD curve of nanodroplets with different number of water molecules on MoS_2 and $MoSe_2$ Films. (c) The process of measuring the contact angle using Fiji ImageJ. (d) to (i) are results of average mass density of water nanodroplet on MoS_2 and $MoSe_2$ Films.

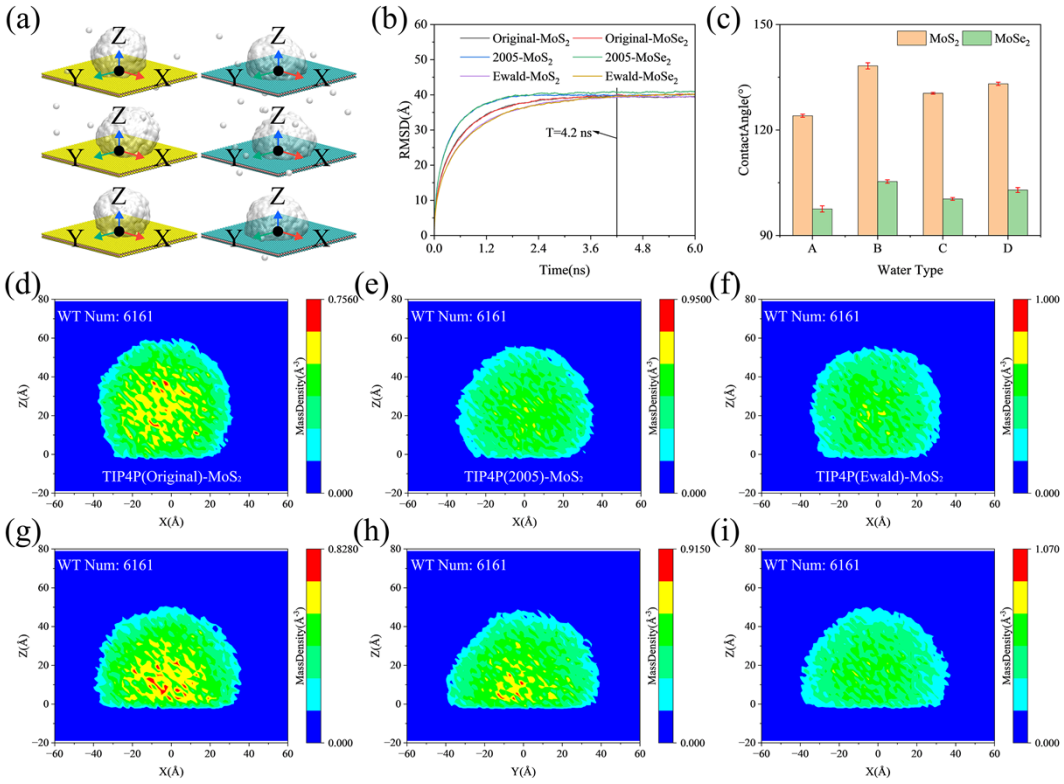

Fig.S8. Measurement of contact angle with TIP4P-seris water models. (a) Schematic diagram of nanodroplets with different number of water molecules on MoS_2 and $MoSe_2$ Films. (b) The RMSD curve of nanodroplets with different number of water molecules on MoS_2 and $MoSe_2$ Films. (c) The contact angles of water nanodroplet on MoS_2 and $MoSe_2$ Films, where type A is TIP3P(Original), type B is TIP4P(Original), type c is TIP4P(2005), and type D is TIP4P(Ewald). (d) to (i) are results of average mass density of water nanodroplet on MoS_2 and $MoSe_2$ Films.

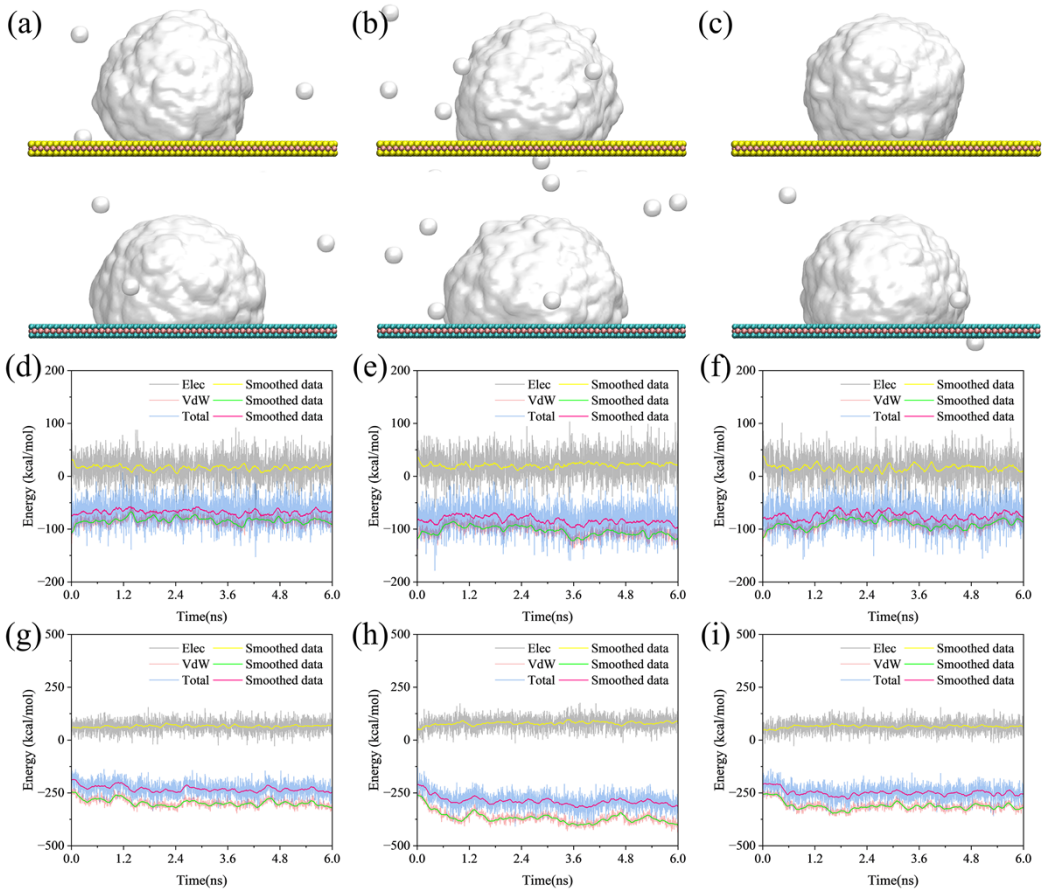

Fig.S9. Interaction energies between water (TIP4P-seris water models) and MoS_2/$MoSe_2$ film. (a) to (c) Schematic diagram of nanodroplets with different model types on MoS_2 and $MoSe_2$ films. (b) The RMSD curve of nanodroplets with different number of water molecules on MoS_2 and $MoSe_2$ films. (d) Interaction energies water (TIP4P-Original) nanodroplet on MoS_2 film. (e) Interaction energies water (TIP4P(2005)) nanodroplet on MoS_2 film. (f) Interaction energies water (TIP4P(Ewald)) nanodroplet on MoS_2 film. (g) Interaction energies of water (TIP4P(Original)) nanodroplet on $MoSe_2$ film. (h) Interaction energies of water (TIP4P(2005)) nanodroplet on $MoSe_2$ film. (i) Interaction energies of water (TIP4P(Ewald)) nanodroplet on $MoSe_2$ film.

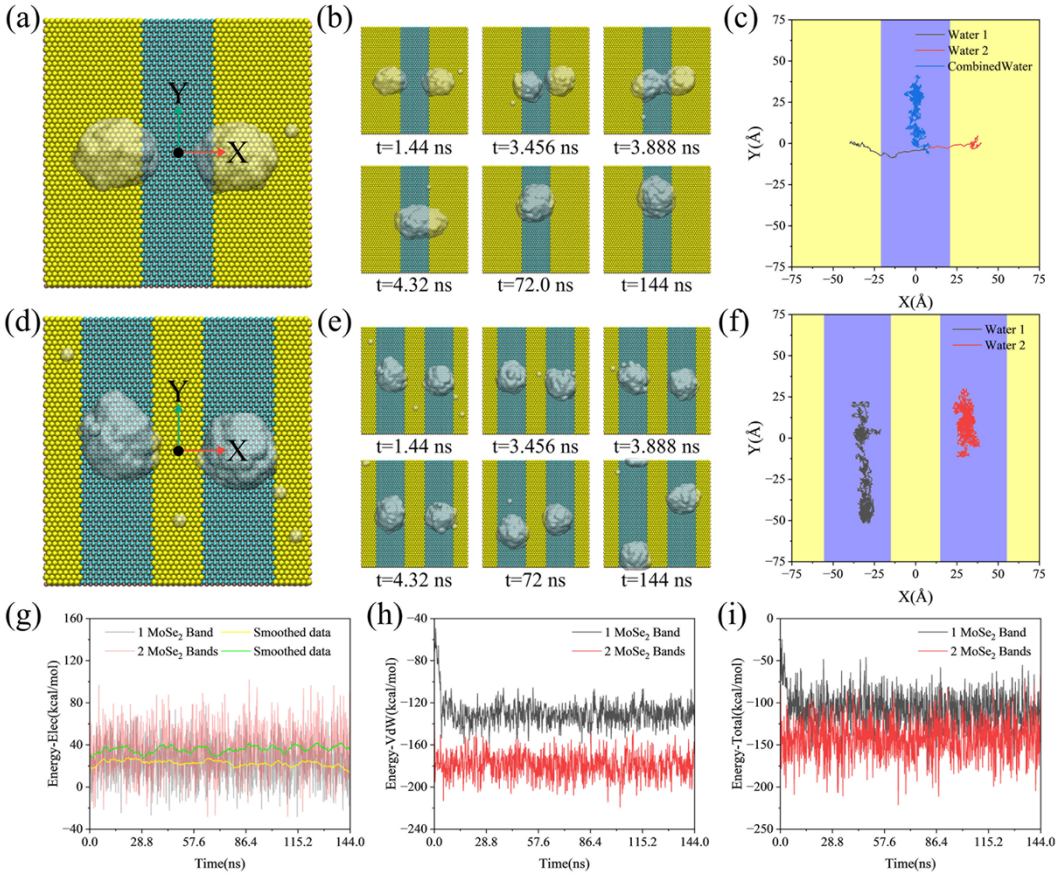

Fig.S10. Enrichment and immobilization of the nanodroplets by designing the $MoS_2/MoSe_2$ heterostructures. (a) Schematic illustration of system setup with two nanodroplets arranged separately on the two sides of the heterostructure with MoS_2 film divided by one $MoSe_2$ strip. (b) Sequence of microscopic configurations of the nanodroplets on the heterostructure realized in a typical MD simulation, the two water nanodroplets gradually merge together. (c) Projection of center of mass of each nanodroplet (before merging) and the merged nanodroplets. (d) Schematic illustration of system setup with two nanodroplets arranged separately on the two strips where the S atoms were modified to Se atoms. (e) Sequence of microscopic configurations of the nanodroplets on the heterostructure realized in a typical MD simulation, the two nanodroplets stay at their own strip. (f) Projection of center of mass of each nanodroplet. (g) Electrostatic interaction energies between the nanodroplet and the heterostructure in panel a and panel d *versus* time. (h) Similar to panel j but for van der Waals interaction energies. (i) Similar to panel j but for total interaction energy.

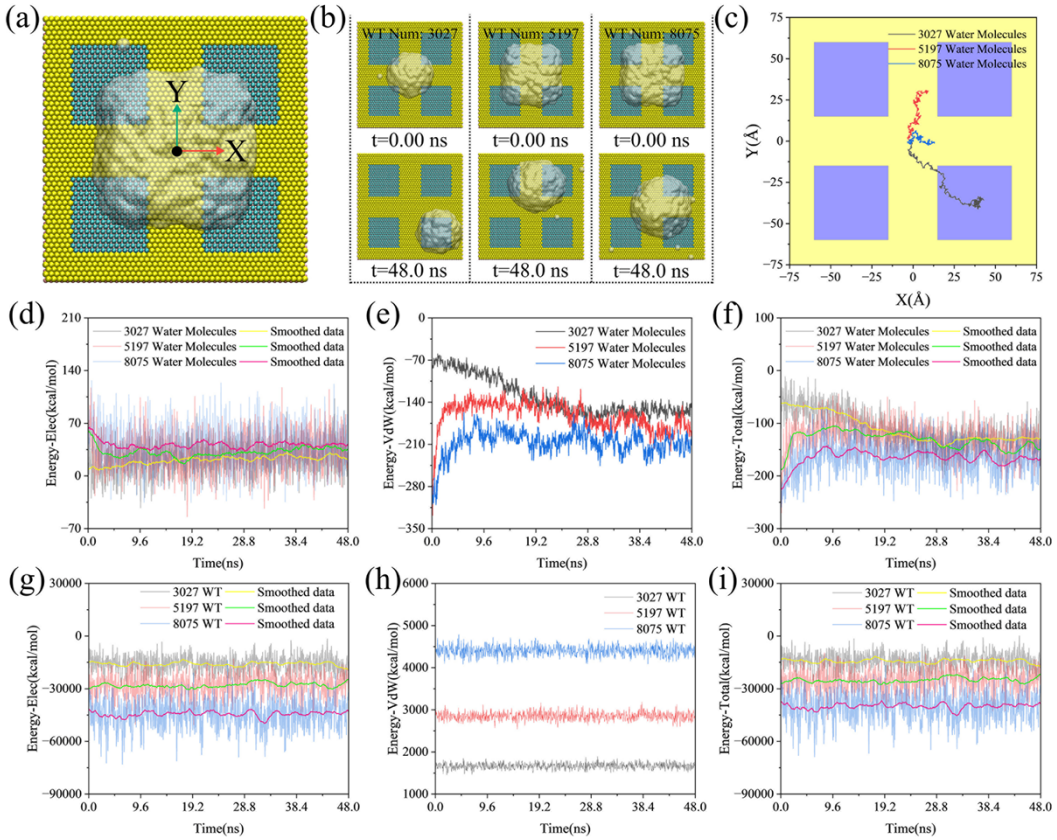

Fig.S11. Investigation on water nanodroplet fission on $MoS_2/MoSe_2$ heterostructures. (a) Schematic illustration of system setup with one large nanodroplets on the middle areas at the film. (b) Sequence of microscopic configurations of the nanodroplets on the heterostructure realized in a typical MD simulation. (c) Projection of center of mass of nanodroplet. (d) Electrostatic interaction energies between the nanodroplet and the heterostructure in panel a *versus* time. (e) Similar to panel d but for van der Waals interaction energies. (f) Similar to panel d but for van der Waals interaction energies. (g) Electrostatic interaction energies inside the nanodroplet in panel a *versus* time. (h) Similar to panel g but for van der Waals interaction energies. (i) Similar to panel g but for total interaction energy.

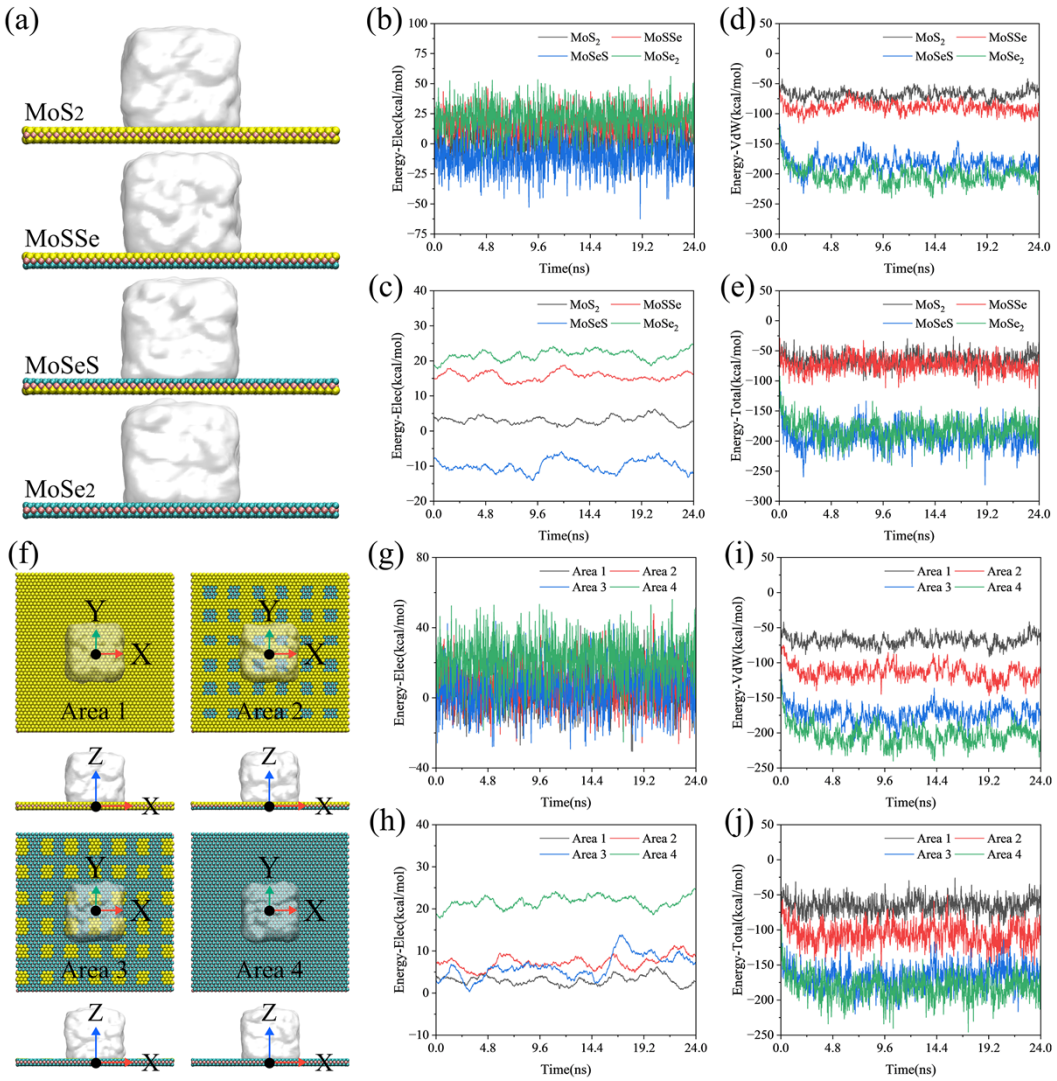

Fig.S12. Interaction behaviors of nanodroplets on different types of TMDs films. (a) Schematic diagram of four different types of TMDs films. (b) Electrostatic interaction energies between the nanodroplet and the heterostructure films *versus* time. (c) Smoothed data of panel b. (d) Similar to panel b but for van der Waals interaction energies. (e) Similar to panel b but for total interaction energies. (f) Schematic diagram of four MoS2/MoSe2 lateral heterostructure films with different wettabilities. (h) Electrostatic interaction energies between the nanodroplet and the heterostructure films *versus* time. (h) Smoothed data of panel g. (i) Similar to panel g but for van der Waals interaction energies. (j) Similar to panel g but for total interaction energies.

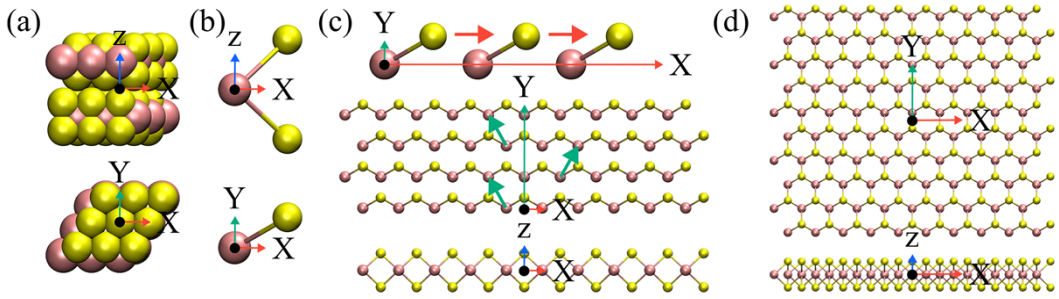

Fig.S13. The process of building 2D $MoS_2/MoSe_2$ film. (a) Schematic diagram of MoS_2 unit cell. (b) Schematic diagram of the basic MoS_2 element for expanding. (c) Expanding the basic element along the x axis and y axis. (d) The final built 2D MoS_2 film.

References

1. M. R. Vazirisereshk, K. Hasz, M.-Q. Zhao, A. T. C. Johnson, R. W. Carpick and A. Martini, ACS Nano, 2020, 14, 16013–16021.
2. L. Yang, L. Sun and W.-Q. Deng, The Journal of Physical Chemistry A, 2018, 122, 1672–1677.
3. Y. Wang, A. Kiziltas, P. Blanchard and T. R. Walsh, Computer Physics Communications, 2021, 266, 108032.
4. C. A. Schneider, W. S. Rasband and K. W. Eliceiri, Nature Methods, 2012, 9, 671–675.